



CrossMark

## Isotherm and Kinetic Evaluation of Acid Blue 80 Dye Adsorption on Surfactant-modified Bentonite

Davoud Balarak <sup>a,\*</sup> | Mohadeseh Dashtizadeh <sup>b</sup> | Hajar Abasizade <sup>b</sup> | Marzieh Baniasadi <sup>b</sup>

<sup>a</sup> Department of Environmental Health, Health Promotion Research Center, Zahedan University of Medical Sciences, Zahedan, Iran.

<sup>b</sup> Department of Environmental Health, Student Research Committee, Zahedan University of Medical Sciences, Zahedan, Iran.

\*Corresponding author: Davoud Balarak

Department of Environmental Health, Health Promotion Research Center, Zahedan University of Medical Sciences, Zahedan, Iran. Tell: +98- 9388517121.

E-mail address: [dbalarak2@gmail.com](mailto:dbalarak2@gmail.com)

### ARTICLE INFO

**Article type:**  
Original article

**Article history:**  
Received March 17, 2018  
Revised April 19, 2018  
Accepted April 25, 2018

DOI: [10.29252/jhehp.4.2.6](https://doi.org/10.29252/jhehp.4.2.6)

**Keywords:**

Adsorption Behavior  
Acid Blue 80  
Isotherms  
Kinetics Words

### ABSTRACT

**Background:** Dyes are among the most hazardous chemical compounds, which are found in industrial effluents. The removal of dyes before the discharge of wastewater to the environment could reduce these environmental hazards. The present study aimed to evaluate the efficiency of cetyltrimethylammonium bromide-modified bentonite (CTAB-MB) surfactant in the adsorption of acid blue 80 (AB80) dye.

**Methods:** This experimental study was conducted using a shaker (100 rpm) at room temperature and fixed pH of 7 using conical flasks (200 ml) containing the dye solution (100 ml) to assess the adsorption conditions. In addition, five concentrations of the reactive blue dye were prepared to evaluate the effects of the initial dye concentration on adsorption.

**Results:** The experimental data indicated that the AB80 removal procedure was fitted with the Langmuir isotherm. The Langmuir adsorption capacities ( $q_e$ ) were 38.15 and 21.76 mg/g for 1 and 2 g/l of the adsorbent, respectively. Moreover, three kinetic models were selected to fit the kinetic data, including the pseudo-first-order and pseudo-second-order models and intra-particle diffusion. AB80 was fitted with the pseudo-second-order model at all the concentrations.

**Conclusion:** According to the results, CTAB-MB was an affordable alternative to the removal of dyes from industrial wastewater.

## 1. Introduction

The disposed dyes in the textile industry cause severe problems in wastewater sources [1, 2]. Dyes are synthetic, water-soluble, dispersible, organic compounds that color natural water bodies when released into the environment [3].

Dyes have a wide range of applications in dyestuff, textile, rubber, leather, paper, plastic, and cosmetic industries for the coloration of the products, and their residues are inevitably found in industrial wastes [4, 5].

Synthetic dyes, suspended solids, and dissolved organics are major hazardous materials in textile effluents, which may affect the physical and chemical properties of fresh water [6-8]. In addition to the undesirable color of textile effluents, some dyes may degrade to produce carcinogens and toxic products [9].

Furthermore, colored effluents reduce light penetration, potentially preventing photosynthesis [10]. Even at low concentrations, synthetic dyes adversely affect the aquatic life and food chain [11].

Therefore, the removal of dyes from industrial processes or waste effluents is environmentally crucial [12].

The removal of dyes from textile wastewater is difficult due to their high water-solubility, complex structure, and synthetic origin [13]. Various physical, chemical, and biological methods have been applied for the removal of dyes from wastewater, including flocculation, coagulation, precipitation, adsorption, membrane filtration, electrochemical techniques, ozonation, and fungal decolorization [14-17]. However, none of these techniques have proven completely successful in the elimination of synthetic dyes from industrial wastewater [18]. Compared to other methods, adsorption is probably one of the simplest, most cost-efficient and effective physical processes for the removal of dyes from wastewater [19, 20].

Activated carbon is an effective adsorbent for the dye adsorption process since it has a high surface area and excellent adsorption capacity, while it is relatively costly and has low selectivity and regeneration problems [21].

Therefore, researchers have been investigating other inexpensive, effective synthetic and natural adsorbents, as well as their modified products; such examples are bentonite (montmorillonite), sepiolite, and zeolite [22, 24].

Bentonite comprises of one octahedral alumina sheet, lying between two tetrahedral layers of silica [25]. The permanent negative charge of bentonite is attributed to the isomorphous replacement of  $Al^{3+}$  for  $Si^{4+}$  in the tetrahedral layer and  $Mg^{2+}$  for  $Al^{3+}$  in the octahedral layer [26]. The negative charge is balanced by the presence of replaceable cations (e.g.,  $Ca^{2+}$  and  $Na^{+}$ ) in the lattice structure, which enhance the adsorption of cationic pollutants. Several studies have been focused on the use of modified and organo-modified bentonite with a cationic surfactant for pollutant elimination via a high load of surfactant [27]. Previous studies have denoted that the main mechanism of the adsorption process in dye elimination is the anionic exchange between the excessive anions and pollutants from the surfactant [26, 27].

In the present study, bentonite was modified using cetyltrimethylammonium bromide (CTAB), which resulted in a new adsorbent and CTAB-modified bentonite (CTAB-MB) to improve the adsorption capacity. CTAB-MB was characterized by scanning electron microscopy (SEM) and nitrogen adsorption measurements. In addition, the adsorption capacity for the removal of acid blue 80 (AB80) was estimated. We also determined the effects of the adsorbent dose, initial concentration, and equilibrium time on the adsorption process in the batch adsorption techniques.

## 2. Materials and Methods

### 2.1. Reagents and Solutions

AB80 has a molecular weight of 678.2 g/mol with the CAS registry number of 4474-24-2, wavelength of 582 nanometers,

and molecular formula of  $C_{32}H_{28}N_2Na_2O_8S_2$ . In the present study, AB80 was purchased from Sigma-Aldrich Company. A stock solution containing 1,000 mg/l of the AB80 was prepared by dissolving the dye in distilled water. Solutions were prepared through the dilution of the stock solution to reach the desired concentrations (10, 20, 30, 40, and 50 mg/L). The stock solutions were refrigerated in a volumetric flask and only taken out for the experiments in order to prevent spoilage. The initial pH of the solutions was measured using a pH-meter (Fisher Scientific Accumet; model: AB15) and adjusted to the required pH value by adding small volumes of hydrochloric acid and sodium hydroxide prior to contact with the adsorbent.

### 2.2. Synthesis of CTAB-MB

CTAB-MB was synthesized in several stages. For CTAB-MB synthesis, 25 grams of bentonite was placed in 250 milliliters of water containing five grams of CTAB. The reaction components were stirred at the temperature of 25°C for 12 hours. The product was filtered and washed with distilled water repeatedly. Afterwards, CTAB-MB was dried at the temperature of 110°C for six hours [25]. The specific surface area of the adsorbents was measured using the Brunauer-Emmett-Teller method and liquid  $N_2$  adsorption at the temperature of 196° K by the conventional volumetric apparatus. The morphology of the sample surfaces was investigated using SEM (JEOL 6400).

### 2.3. Batch Experiments

Batch adsorption experiments were conducted on a shaker at 100 rpm at room temperature using conical flasks (200 ml) containing 100 milliliters of the dye solution in order to assess the effects of the adsorption conditions at the fixed pH of 6.8-7. To evaluate the effects of the initial dye concentration, five concentrations of the AB80 dye (10, 20, 30, 40, and 50 mg/l) were prepared. Moreover, the effects of the adsorbent were determined using the adsorbent concentrations of 0.04, 0.08, 0.1, 0.15, 0.2, 0.25, 0.3, and 0.4 g/100 ml .

After the adsorption process, the solution was centrifuged for 10 minutes at 6,000 rpm, and the supernatants were studied in terms of the remaining dye concentrations using a UV-1800 spectrophotometer (Shimadzu) at each dye wavelength. Finally, the adsorption capacity and removal rate (in percentage) were calculated using the mass balance equation for the adsorbent, as follows [28, 29]:

$$q_e = \frac{(C_0 - C_e)V}{m}$$

$$\% R = \frac{(C_0 - C_e)}{C_0} \times 100$$

Where,  $C_0$  and  $C_e$  represent the initial and equilibrium concentrations of AB80 (mg/l) in the solution,  $q_e$  denotes the adsorption capacity (mg/g),  $V$  is the volume of the AB80 solution (l), and  $W$  shows the adsorbent weight (g).

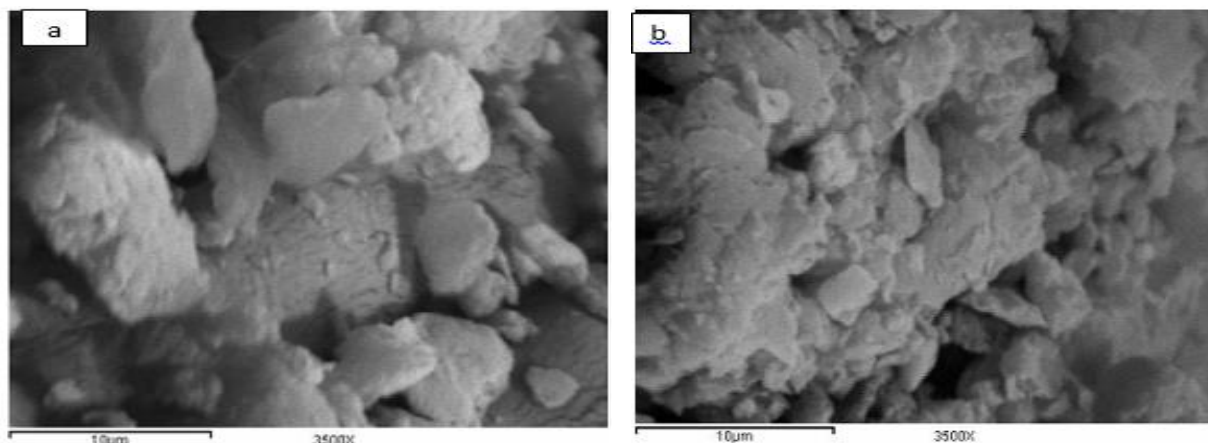


Figure 1: SEM micrographs of a: Bentonite b: surfactant-modified

### 3. Results and Discussion

#### 3.1. Characterization of Bentonite and CTAB-MB

The specific surface area and porosity are the foremost characteristics of adsorbents. In the present study, the specific surface area and pore volume were estimated at  $49.8 \text{ m}^2/\text{g}$  and  $0.016 \text{ ml/g}$ , respectively. The SEM images of bentonite and MB are depicted in Figures 1-a and 1-b. As can be seen, the bentonite agglomerates contained a few particles compared to those of MB. In addition, several particles in bentonite and MB showed the laminar crystalline habit characteristics of phyllosilicates. However, these particles were more dominant in MB compared to bentonite.

The interactions of the surfactant molecules in the interlayer may also be attributed to the domination of the comparatively large laminar crystallites and agglomerates [28].

#### 3.2. Effects of the Adsorbent Dosage

Adsorbent dosage is a significant influential factor in the adsorption process since it affects the adsorption capacity of the adsorbent [30]. The effects of the adsorbent dosage on AB80 removal is illustrated in Figure 2. According to the results of the present study, increased adsorbent dosage from 0.05 to 0.4 g/100 ml led to a higher rate of AB80 removal (from 35.5% to 87.68%). Furthermore, the adsorption of Cr enhanced rapidly with the increased dosage of the adsorbent from 0.05 to 0.1 gram, followed by a slight enhancement from 0.1 to 0.2 gram. This could be attributed to the increased sorbent surface area and availability of more adsorption sites. However, our findings indicated that the adsorption capacity decreased with the increased adsorbent dosage at constant dye concentrations (Figure 2), which could be attributed to the saturation of the adsorption sites on the adsorbent surface due to particulate interactions which could be attributed to the

saturation of the adsorption sites on the adsorbent surface due to particulate interactions (e.g., aggregation and aggregation), which led to the reduction of the total surface area of the adsorbent.

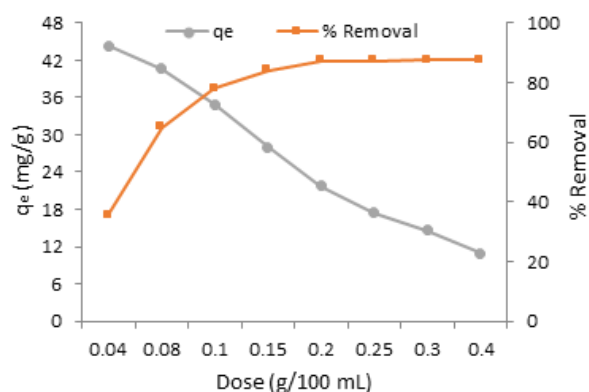


Figure 2: The effect of adsorbent dosage on AB-80 removal ( $C_0=50 \text{ mg/L}$ ;  $\text{pH}=7$ ;  $\text{time}=75 \text{ min}$ )

#### 3.3. Adsorption Kinetics

The kinetics of adsorption for the prepared CTAB-MB was desirable to determine whether the behavior of dye adsorption on the adsorbents could be described by a predictive theoretical model. Figure 3 shows the results of the time-dependent AB80 adsorption performance of the CTAB-MB. Accordingly, the adsorption was an extremely quick process. The adsorption rate increased rapidly within the first 30 minutes, contributing to approximately 75% of the ultimate adsorption amount, which augmented gradually afterwards and approached the adsorption equilibrium within 75 minutes. Such adsorption behaviors are typical of the specific adsorption process, where the adsorption rate often depends on the number of the available adsorption sites on the adsorbent surface, which is eventually controlled by the attachment of the dye ions to the surface.

In the current research, adsorption kinetic models were applied to interpret the experimental data in order to determine the controlling mechanism of AB80 adsorption from aqueous solutions. In this regard, we used Lagergren pseudo-first-order and Ho and McKay pseudo-second-order models to assess the dynamic, experimental data. Lagergren pseudo-first-order kinetic is as follows:

$$\text{Log}(q_e - q_t) = \text{log } q_e - \frac{K_1}{2.303}t$$

Where  $q_t$  is the amount of the adsorbed AB80 per unit of the adsorbent (mg/g) at the time  $t$ , and  $K_1$  represents the pseudo-first-order rate constant ( $\text{min}^{-1}$ ). The adsorption rate constant ( $K_1$ ) was calculated based on the log plot ( $q_e - q_t$ ) against  $t$ .

Ho and McKay presented the pseudo-second-order kinetic, as follows:

$$\frac{t}{q_t} = \frac{1}{k_2 q_e^2} + \frac{t}{q_e}$$

Plots of  $t/q_t$  versus  $t$  which are illustrated in Figure 4. The calculated parameters are presented in Table 1. According to the information in this table, the correlation-coefficients for the pseudo-first-order kinetic model were comparatively lower, and the  $q_e$  cal was significantly deviated from the  $q_e$  exp data, which suggested that the adsorption system was the pseudo-second-order kinetic adsorption process. This is because in many cases, the pseudo-first-order equation is not well-fitted to the whole range of the contact time and is applicable only in the initial stage of the adsorption process.

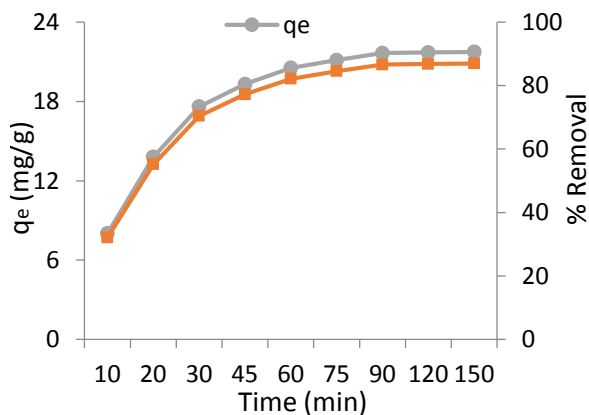


**Figure 3:** Effect of contact time on the removal of AB-80  
 $C_o=50 \text{ mg/L}$ ;  $\text{pH}=7$ ; dose;  $0.2 \text{ g/100 (mL)}$

### 3.5. Adsorption Mechanism

The adsorption mechanism of the adsorbate onto the adsorbent followed three steps, including film diffusion, pore diffusion, and intraparticle transport. Furthermore, the effect of intraparticle diffusion on the adsorption rate was calculated

based on the correlation between the adsorption capacity and time, which is normally expressed as follows:

$$q_t = K_d t^{0.5} + C$$

Where  $q_t$  denotes the amount of the adsorbed dye at any time (mg/g),  $K_d$  is the intraparticle diffusion rate constant ( $\text{mg/g min}^{0.5}$ ), and  $C$  represents the intercept of the straight lines, which provides the data on the boundary layer thickness. With regard to the fitting data to the mentioned equation, our findings demonstrated that if the linear correlation value is close to unity, the intraparticle diffusion process is effective in CTAB-MB. Figure 5 illustrates the intraparticle diffusion curves for AB80 adsorption. As can be seen, the adsorption process was followed by two phases, and the resulting fitting line did not pass through the origin. Moreover, an initial linear portion ended with a smooth curve, followed by another linear curve. The two phases in the intraparticle diffusion plot suggested that the adsorption process occurred through surface adsorption, as well as the intraparticle diffusion. The initial curved portion of the plot was rapid, demonstrating the effect of the boundary layer, while the second linear portion was due to intraparticle or pore diffusion.

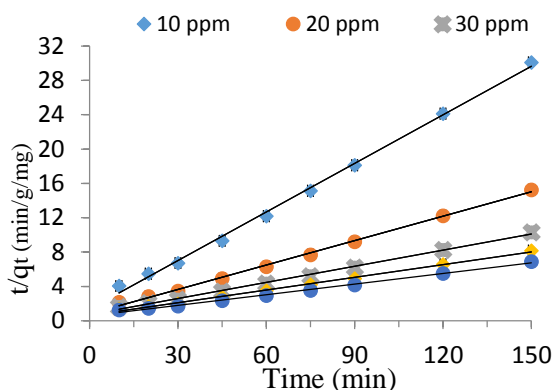


**Figure 4:** Pseudo- second-order kinetic model for the adsorption of AB-80 dye

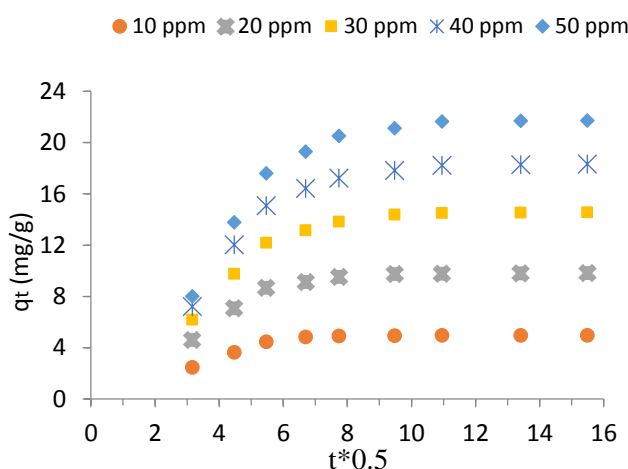


**Figure 5:** Intraparticle diffusion kinetics of AB-80 dye adsorption CTAB-MB

**Table 1:** The results of kinetic model studies related to the AB-80 adsorption onto CTAB-MB

AMO Concentration (mg/L)	(qe) exp	Intraparticle diffusion model			Pseudo-first order			Pseudo-second order		
		K	C	R <sup>2</sup>	(qe) cal	K	R <sup>2</sup>	(qe) cal	K	R <sup>2</sup>
10	4.96	0.919	10.38	0.727	0.941	0.241	0.925	3.85	0.0097	0.998
20	9.45	0.718	9.494	0.704	4.36	0.189	0.907	8.94	0.0081	0.997
30	13.65	0.542	7.932	0.691	7.95	0.146	0.923	13.08	0.0063	0.999
40	17.34	0.321	5.961	0.689	10.74	0.117	0.932	17.11	0.0044	0.998
50	21.73	0.151	3.182	0.687	14.61	0.094	0.917	20.91	0.0017	0.997

**Table 2:** Isotherms constants for the removal AB-80 onto CTAB-MB

Adsorbent dose (g/L)	Langmuir model				Freundlich model		
	q <sub>m</sub>	R <sub>L</sub>	K <sub>L</sub>	R <sup>2</sup>	n	K <sub>F</sub>	R <sup>2</sup>
1	38.15	0.023	0.824	0.997	1.19	7.417	0.911
2	21.76	0.032	0.601	0.998	2.55	9.602	0.882

### 3.6. Adsorption Isotherms

The equilibrium adsorption isotherm was used to describe the amount of the adsorbed adsorbate on the adsorbent and concentration of the dissolved adsorbate at the equilibrium. In addition, the Langmuir and Freundlich isotherms were expressed using the following equations:

$$\frac{C_e}{q_e} = \frac{1}{q_m K_L} + \frac{C_e}{q_m}$$

$$\text{Log} q_e = \log K_F + \frac{1}{n} \text{Log} C_e$$

Where  $C_e$  is the equilibrium concentration of AB80 (mg/l),  $q_e$  represents the amount of the sorbed AB80 on the CTAB-MB (mg/g),  $K_L$  denotes the constant of the Langmuir model (mg/L),  $q_{\text{max}}$  is the maximum sorbed AB80 by the CTAB-MB,  $K_F$  shows the Freundlich adsorption constant, and the constant  $n$  is the empirical parameter associated with the adsorption intensity, which varies with material heterogeneity. When  $1/n$  values are within the range of  $0.1 < 1/n < 1$ , the adsorption process is considered to be favorable.

The plot of the experimental  $C_e/q_e$  against  $C_e$  and  $\log q_e$  against  $\log C_e$  yields the  $1/q_{\text{max}}$  slope. Moreover, the intercept  $1/K_L q_{\text{max}}$  and  $1/n$  and  $\log K_F$  values were calculated based on the slope and intercept of the  $\log q_e$  plot against  $\log C_e$ , for the experimental data (figures are not shown).

These figures show the Langmuir and Freundlich curves for AB80 adsorption on CTAB-MB, along with the experimental data.

The Langmuir and Freundlich constants and correlation-coefficients are presented in Table 2. Based on the obtained coefficients, it could be concluded that the Langmuir equation had a better fit for the experimental data (e.g., 0.997 and 0.998 for 1 and 2 g/l of CTAB-MB, respectively) compared to the Freundlich equation. Therefore, the Langmuir isotherm had a better correlation with the experimental data compared to the Freundlich isotherm.

The  $1/n$  values at the equilibrium were within the range of 0.391-0.836, indicating a favorable adsorption. This finding

suggested the dominance of a physical mechanism when used for AB80 adsorption, which demonstrated that the adsorption bond became weak with the van der Waals forces rather than chemical adsorption. The obtained data indicated that AB80 adsorption on CTAB-MB could be well-fitted to the Langmuir isotherm model compared to the Freundlich isotherm model.

## 4. Conclusion

The present study aimed to describe the adsorption of the AB80 dye from aqueous solutions using CTAB-MB.

According to the experimental results, the maximum removal efficiency of the AB80 ions occurred at the initial concentration of 10 mg/l and contact time of 75 minutes. Additionally, the removal efficiency of the AB80 ions increased at the higher dosage of the adsorbent. On the other hand, the isotherm study indicated that the Langmuir isotherm could optimally model the adsorption process.

Finally, our findings suggested that CTAB-MB is a suitable sorbent material for the adsorption of AB80 from aqueous solutions.

## Authors' Contributions

D.B., designed the interviews forms for all sectors with M.D., collaboration and conducted the interview. H.A., did interviews, analyzed data and wrote the manuscript. M.D., conducted the study and revised the manuscript. M.B., helped and analyzed the statistical data. All authors revised and approved the final manuscript.

## Conflict of Interest

The authors affirm that there is no conflicts of interest that may have influenced the preparation of this manuscript.

## Acknowledgments

Hereby, we extend our gratitude to the Student Research Committee of Zahedan University of Medical Sciences for supporting this research project.

## References

1. Qiu M, Qian C, Xu J, Wu J, Wang G. Studies on the Adsorption of dyes into Clinoptilolite. *Desalination*. 2009; 243: 286-92.
2. Wang XS, Zhou Y, Jiang Y, Sun C. The Removal of Basic dyes from Aqueous Solutions Using Agricultural by-Products. *J Hazard Mater*. 2008; 157: 374-85.
3. Balarak D, Mahdavi Y, Bazrafshan E, Mahvi AH. Kinetic, Isotherms and Thermodynamic Modeling for Adsorption of Acid blue 92 from Aqueous Solution by Modified Azolla Filiculoides. *Fresenius Environmental Bulletin*. 2016; 25(5): 1321-30.
4. Balarak D, Mahdavi Y, Kord Mostafapour F, Azarpira H. Using of Lemna Minor for Adsorption of Acid Green 3 dye (AG3) from Aqueous Solution: Isotherm and Kinetic Study. *J Chem Mater Res*. 2016; 5 (5): 92-8.
5. Garg VK, Gupta R, Yadav AB, Kumar R. Dye Removal from Aqueous Solution by Adsorption on Treated Sawdust. *Bioresour Technol*. 2003; 89(2): 121-4.
6. Senthilkumaar S, Varadarajan PR, Porkodi K, Subbhuraam CV. Adsorption of Methylene Blue onto Jute Fiber Carbon: Kinetics and Equilibrium Studies. *J Colloid Interface Sci*. 2005; 284: 78-82.
7. Kumar PS, Ramalingam S, Senthamarai C, Niranjana M. Adsorption of dye from Aqueous Solution by Cashew Nut Shell: Studies on Equilibrium Isotherm, Kinetics and Thermodynamics of Interactions. *Desalination*. 2010; 261: 52-60.
8. Yan C, Wang C, Yao J, Zhang L, Liu X. Adsorption of Methylene Blue on Mesoporous Carbons Prepared Using Acid- and Alkaline-Treated Zeolite X as the Template. *Colloids Surf A Physicochem Eng Asp*. 2009; 333(1-3): 115-9.
9. Padmesh TVN, Vijayaraghavan K, Sekaran G, Velan M. Application of Azolla Rongpong on Biosorption of Acid Red 88, Acid Green 3, Acid Orange 7 and Acid Blue 15 from Synthetic Solutions. *Chem Eng J*. 2006; 122(1-2): 55-63.
10. Balarak D, Mahdavi Y, Sadeghi S. Adsorptive Removal of Acid Blue 15 Dye (AB15) from Aqueous Solutions by Red Mud: Characteristics, Isotherm and Kinetic Studies Scientific. *J Environ Sci*. 2016; 4(5): 102-12.
11. Asouhidou DD, Triantafyllidis KS, Lazaridis NK, Matis KA, Kim SS. Sorption of Reactive Dyes from Aqueous Solution by Ordered Hexagonal and Disordered Mesoporous Carbons. *Micropor Mesopor Mater*. 2009; 117: 257-67.
12. Jin X, Jiang M, Shan X, Pei Z, Chen Z. Adsorption of Methylene Blue and Orange II onto Unmodified and Surfactant-Modified Zeolite. *J Colloid Interf Sci*. 2008; 328: 243-7.
13. Gök O, Özcan AS, Özcan A. Adsorption Behavior of a Textile Dye of Reactive Blue 19 from Aqueous Solutions onto Modified Bentonite. *Appl Surf Sci*. 2010; 256: 5439-43.
14. Ceyhan O, Baybas D. Adsorption of Some Textile Dyes by Hexadecyltrimethyl Ammonium Bentonite. *TURK J Chem*. 2001; 25: 193-200.
15. Jovic-Jovicic N, Milutinovic-Nikolic A, Grzetic I, Jovanovic D. Organobentonite as Efficient Textile Dye Sorbent. *Chem Eng Technol*. 2008; 31: 567-74.
16. Ozcan AS, Erdem B, Ozcan A. Adsorption of Acid Blue 193 from Aqueous Solutions onto Na-bentonite and DTMA-Bentonite. *J Colloid Interface Sci*. 2004; 280: 44-54.
17. Ozcan AS, Ozcan A. Adsorption of Acid Dyes from Aqueous Solutions onto Acid-Activated Bentonite. *J Colloid Interface Sci*. 2004; 276: 39-46.
18. Zohra B, Aicha K, Fatima S, Nourredine B, Zoubir D. Adsorption of Direct Red 2 on Bentonite Modified by Cetyltrimethylammonium Bromide. *Chem Eng J*. 2008; 136: 295-305.
19. Sanghi R, Bhattacharya B. Review on Decolorisation of Aqueous Dye Solutions by Low Cost Adsorbents. *Color Technol*. 2002; 118: 256-69.
20. Kara S, Aydiner C, Demirbas E, Kobya M, Dizge N. Modeling the Effects of Adsorbent dose and Particle Size on the Adsorption of Reactive Textile Dyes by Fly Ash. *Desalination*. 2007; 212: 282-93.
21. Balarak D, Bazrafshan E, Kord Mostafapour F. Equilibrium, Kinetic Studies on the Adsorption of Acid Green 3 (Ag3) Dye onto Azolla Filiculoides as Adosorbent. *Am Chem Sci J*. 2016; 11(1): 1-10.
22. Chiou MS, Ho PY, Li HY. Adsorption of Anionic Dyes in Acid Solutions Using Chemically Cross-Linked Chitosan Beads. *Dyes Pigm*. 2004; 60: 69-84.
23. Anirudhan TS, Ramachandran M. Surfactant-Modified Bentonite as Adsorbent for the Removal of Humic Acid from Wastewaters. *Appl Clay Sci*. 2007; 35: 276-81.
24. Bhattacharyya KG, Sarma A. Adsorption Characteristics of the Dye, Brilliant Green, on Neem Leaf Powder. *Dyes Pigm*. 2003; 57: 211-22.
25. Lagergren SK. About the Theory of So-called Adsorption of Soluble Substances. *Kungliga Svenska Vetenskapsakademiens Handlingar*. 1898; 24: 1-39.
26. Ho YS, McKay G. Pseudo-Second order Model for Sorption Processes. *Process Biochem*. 1999; 34: 451-65.
27. Hameed BH, Ahmad AA. Batch Adsorption of Methylene Blue from Aqueous Solution by Garlic Peel, an Agricultural Waste Biomass. *J Hazard Mater*. 2009; 164: 870-5.
28. Balarak D, Joghataei A, Azadi NA, Sadeghi S. Biosorption of Acid Blue 225 from Aqueous Solution by Azolla Filiculoides: Kinetic and Equilibrium Studies. *Am Chem Sci J*. 2016; 12 (2), 1-10.
29. Sismanoglu T, Kismir Y, Karakus S. Single and Binary Adsorption of Reactive Dyes from Aqueous Solutions onto Clinoptilolite. *J Hazard Mater*. 2010; 184: 164-9.
30. Karadag D, Turan M, Akgul E, Tok S, Faki A. Adsorption Equilibrium and Kinetics of Reactive Black 5 and Reactive Red 239 in Aqueous Solution onto Surfactant-Modified Zeolite. *J Chem Eng Data*. 2007; 52: 1615-20.